Quantum Fisher information and spin squeezing in one-axis twisting model*

Zhong Wei(钟 伟), Liu Jing(刘 京), Ma Jian(马 健), and Wang Xiao-Guang(王晓光)†

Zhejiang Institute of Modern Physics, Zhejiang University, Hangzhou 310027, *China*

(Received 3 December 2013; revised manuscript received 20 February 2014; published online 10 April 2014)

We investigate the dependence of the average parameter estimation precision (APEP), which is defined by the quantum Fisher information, on the polar angle of the initial coherent spin state $|\theta_0, \phi_0\rangle$ in a one-axis twisting model. Jin *et al.* [*New J. Phys.* **11** (2009) 073049] found that the spin squeezing sensitively depends on the polar angle θ_0 of the initial coherent spin state. We show explicitly that the APEP is robust to the initial polar angle θ_0 in the vicinity of $\pi/2$ and a near-Heisenberg limit $\propto 2/N$ in quantum single-parameter estimation may still be achieved for states created with the nonlinear evolution of the nonideal coherent spin states $\theta_0 \sim \pi/2$. Based on this model, we also consider the effects of the collective dephasing on spin squeezing and the APEP.

Keywords: quantum Fisher information, spin squeezing, one-axis twisting model

PACS: 03.65.Yz, 06.20.–f, 42.50.Dv **DOI:** 10.1088/1674-1056/23/6/060302

1. Introduction

Fisher information, a key notion in statistical inference, was first proposed by Fisher in 1925.[1] It is used to quantify the amount of the information that one can extract about a parameter from the observed probability distribution. Moving into the quantum regime, its counterpart is known as the quantum Fisher information (QFI), which gives the theoretical achievable limit on the measurement precision in quantum metrology.[2–5] Recently, QFI has attracted much attention in the modern science of quantum information because it is closely related to fidelity,[4,6,7] nonclassicality,[8,9] multipartite entanglement,[10,11] and non-Markovianity.[12,13] It has also been shown that the QFI can be used to characterize quantum chaos[14,15] and phase transitions.[16,17] In Ref. [10], Pezze *et al.* provided a sufficient condition for particle entanglement based on the QFI as

$$\chi^2 \equiv \frac{N}{\mathcal{F}_\varphi} < 1, \tag{1}$$

where $\mathcal{F}_\varphi$ denotes the QFI in terms of a parameter φ containing in quantum states and N is the total number of particles; that is, atoms and photons. According to quantum Cramér–Rao theorem,[2–5] the accuracy of estimation is asymptotically bounded by the inverse of QFI (see Eq. (16) below). Thus, the quantity χ^2 in Eq. (1) is the average parameter estimation precision (APEP) normalized by the maximum parameter estimation precision of unentangled states. Equation (1) shows that a quantum state with the APEP-enhancing must be entangled.

Spin squeezed states (SSSs), which can be also used to improve the accuracy of estimation,[10,18–21] are one type of quantum entangled states. The concept of spin squeezing was first established by Kitagawa and Ueda.[22] They also gave the specific schemes to generate the SSSs, such as one-axis twisting (OAT)[23–25] and two-axis counter-twisting (TAT).[26] Moreover, there are many other promising mechanisms to produce SSSs.[27–32] In Ref. [23], Jin *et al.* investigated the dependence of the spin squeeze on the polar angle θ_0 of the initial coherent spin state (CSS) $|\theta_0, \phi_0\rangle$ in the OAT model and found that, for a small departure of θ_0 from $\pi/2$, the achievable variance $(V_{\min}) \sim N^{2/3}$ is larger than the ideal case $N^{1/3}$.

In this paper, we investigate the dependence of the APEP on the initial polar angle θ_0 and the initial azimuth angle ϕ_0 in the OAT model. We first derive the analytical expression of the QFI in the OAT model with an initial CSS $|\theta_0, \phi_0\rangle$. We find that the APEP is independent of the initial azimuth ϕ_0, the same as the spin squeezing.[23] Unlike the spin squeezing, we find that the APEP is insensitive to the initial angle θ_0 in the vicinity of $\pi/2$. Our result shows that, even for states created with the OAT-Hamiltonian evolution of non-ideal initial CSSs $\theta_0 \sim \pi/2$, the near-Heisenberg-scaling sensitivity $\propto 2/N$ may still be achieved. It was demonstrated that such sensitivity can be reached by the SSS generated from the ideal initial CSS $\theta_0 = \pi/2$.[10] In addition, decoherent processes are taken into account in this model. We discuss the influence of collective dephasing[33–35] on the APEP and spin squeezing. Our results show that both the spin squeezing and the APEP are diminished as a result of the collective dephasing, which is consistent with that given in Ref. [36]. We find that, at the expense of an amount of the evolution time, the near-Heisenberg-scaling sensitivity may also be reached even in the presence of collec-

*Project supported by the National Basic Research Program of China (Grant No. 2012CB921602) and the National Natural Science Foundation of China (Grant Nos. 11025527 and 10935010).

†Corresponding author. E-mail: xgwang@zimp.zju.edu.cn

© 2014 Chinese Physical Society and IOP Publishing Ltd

tive dephasing.

The outline of this paper is arranged as follows. In Section 2, we give the notations and definitions of the QFI and spin squeezing. In Section 3, we devote to considering the maximal QFI and spin squeezing in the OAT model and derive the analytical results. Then, we make a comparison between the APEP χ^2 and spin squeezing parameter $\xi_{\rm W}^2$. In Section 4, we consider the effects of the collisional dephasing on χ^2 and $\xi_{\rm W}^2$. Finally, we make a conclusion in Section 5.

2. Quantum Fisher information and spin squeezing

In this section, we briefly recall two key definitions. We first introduce the definition of the QFI and the formula for calculation of the maximal QFI. Secondly, we review the two kinds of spin squeezing parameters.

2.1. Quantum Fisher information

Quantum Fisher information gives the fundamental limit to the accuracy of estimating an unknown parameter, playing a paramount role in quantum metrology.[4] Its classical counterpart in the statistical inference is defined as follows. Given a parameterized family of condition probability densities $p(\varepsilon|\varphi)$ conditioned on parameter $\varphi \in \mathbb{R}$, the classical Fisher information with respect to φ is defined as

$$F_\varphi := \int_{\mathbb{R}} \left(\frac{\partial \ln p(\varepsilon|\varphi)}{\partial \varphi} \right)^2 p(\varepsilon|\varphi)\, {\rm d}\varepsilon, \tag{2}$$

where ε denotes the measurement outcomes of an observable random variable E. Note that the observable E here is a continuous variable. If it is discrete, the integral in Eq. (2) is replaced by a summation. Equation (2) shows that the classical Fisher information is expressed as a statistical variance of a ε-dependent estimator defined by the logarithmic derivative of $p(\varepsilon|\varphi)$; that is, $L_{\rm cl} \equiv \partial\,[\ln p(\varepsilon|\varphi)]/\partial\varphi$.

In the quantum setting, the QFI is defined by

$$\mathcal{F}_\varphi = {\rm Tr}\left(\rho_\varphi L_\varphi^2\right), \tag{3}$$

where L_φ is the symmetric logarithmic derivative (SLD) operator L_φ, which is defined by the following equation

$$\frac{\partial}{\partial\varphi}\rho_\varphi = \frac{1}{2}\left(L_\varphi\rho_\varphi + \rho_\varphi L_\varphi\right). \tag{4}$$

From the above equation, we have $L_\varphi^\dagger = L_\varphi$ and ${\rm Tr}(\rho_\varphi L_\varphi) = 0$. Thus, the QFI of Eq. (3) can be known as the variance of L_φ on the state ρ_φ.

In the most fundamental parameter estimation task, the parameter φ to be estimated may be generated via some unitary[37] or non-unitary dynamics.[38,39] In this paper, we only focus on the unitary case in which the parametrization process is expressed as

$$\rho_\varphi = \exp(-{\rm i}\varphi J_{\boldsymbol{n}})\,\rho_{\rm in}\exp({\rm i}\varphi J_{\boldsymbol{n}}), \tag{5}$$

where $J_{\boldsymbol{n}}$ denotes the collective angular momentum in $\boldsymbol{n}$ direction with

$$J_{\boldsymbol{n}} = \boldsymbol{J}\cdot\boldsymbol{n} = \sum_{\alpha=x,y,z} J_\alpha n_\alpha. \tag{6}$$

The components of the collective angular momentum are given by

$$J_\alpha = \sum_{k=1}^{N} \frac{\sigma_{k\alpha}}{2}, \tag{7}$$

where $\sigma_{k\alpha}$ denotes the Pauli matrix acting on the k-th particle. Here, the unitary process given by Eq. (5) may be used to model the two-mode optical interferometry and the standard Ramsey interferometry.[10,40] With Eq. (5), the QFI with respect of φ can be expressed in the following form[41]

$$\mathcal{F}_\varphi = \boldsymbol{n}\boldsymbol{C}\boldsymbol{n}^{\rm T}, \tag{8}$$

where $\boldsymbol{C}$ is a symmetry matrix with the matrix elements given by

$$C_{\alpha,\beta} = \sum_{i\neq j} \frac{(p_i - p_j)^2}{p_i + p_j} |\langle i|J_\alpha|j\rangle\langle i|J_\beta|j\rangle + \langle i|J_\beta|j\rangle\langle i|J_\alpha|j\rangle|^2, \tag{9}$$

where λ_i and $|i\rangle$ are the eigenvalues and eigenvectors of $\rho_{\rm in}$, respectively. For pure states (i.e., $\rho_\varphi^2 = \rho_\varphi$) the QFI is simply expressed as

$$\mathcal{F}_\varphi = 4\Delta J_{\boldsymbol{n}}^2. \tag{10}$$

Corresponding to Eq. (9), the matrix elements of $\boldsymbol{C}$ can be written in the covariance form

$$C_{\alpha,\beta} = {\rm Cov}\left\langle J_\alpha, J_\beta\right\rangle \equiv \frac{1}{2}\left[\langle J_\alpha J_\beta\rangle + \langle J_\beta J_\alpha\rangle\right] - \langle J_\alpha\rangle\langle J_\beta\rangle. \tag{11}$$

To obtain the maximal QFI, we rewrite the variance as[41]

$$\Delta J_{\boldsymbol{n}}^2 = \boldsymbol{n}\boldsymbol{O}(\boldsymbol{O}^{\rm T}\boldsymbol{C}\boldsymbol{O})\boldsymbol{O}^{\rm T}\boldsymbol{n}^{\rm T} = \tilde{\boldsymbol{n}}\boldsymbol{C}_{\rm d}\tilde{\boldsymbol{n}}^{\rm T}, \tag{12}$$

where $\boldsymbol{O}$ is an orthogonal matrix, $\tilde{\boldsymbol{n}}$ denotes the rotated direction as $\tilde{\boldsymbol{n}} = \boldsymbol{n}\boldsymbol{O}$, and $\boldsymbol{C}_{\rm d}$ is the diagonal form of $\boldsymbol{C}$,

$$\boldsymbol{C}_{\rm d} = \boldsymbol{O}^{\rm T}\boldsymbol{C}\boldsymbol{O} = {\rm diag}\{\lambda_i, \lambda_2, \lambda_3\}, \tag{13}$$

where λ_i are the eigenvalues of $\boldsymbol{C}$. Furthermore, equation (12) can be expressed as

$$\max(\Delta J_{\boldsymbol{n}}^2) = \max(\lambda_1\tilde{n}_1^2 + \lambda_2\tilde{n}_2^2 + \lambda_3\tilde{n}_3^2). \tag{14}$$

In the above equation, the rotated direction is normalized and satisfies the condition $\tilde{n}_1^2 + \tilde{n}_2^2 + \tilde{n}_3^2 = 1$. Assuming that $\lambda_{\rm max} = \lambda_1$ as the maximal eigenvalue, we then obtain

$$\mathcal{F}_{\varphi,\rm max} = 4\lambda_{\rm max}, \tag{15}$$

with $\tilde{\boldsymbol{n}} = (1,0,0)$ and the original direction $\boldsymbol{n} = \tilde{\boldsymbol{n}}\boldsymbol{O}^{\mathrm{T}}$.[41]

According to quantum Cramér–Rao theorem,[2–5] for υ repetitions of an experiment and any locally unbiased estimator $\hat{\varphi}$, the sensitivity of estimation is bounded by the following inequality

$$\Delta\hat{\varphi} \geq \Delta\varphi_{\mathrm{QCRB}} = \frac{1}{\sqrt{\upsilon \mathcal{F}_{\varphi}}}, \tag{16}$$

where the equality is saturated in the asymptotic limit $\upsilon \to \infty$ and $\Delta\varphi_{\mathrm{QCRB}}$ is the so-called quantum Cramér–Rao bound (QCRB). With Eq. (1), equation (16) can be rewritten as

$$\Delta\varphi_{\mathrm{QCRB}} = \frac{\chi}{\sqrt{\upsilon N}}. \tag{17}$$

This shows that when the state is entangled then $\chi^2 \leq 1$, which means that this state can suppress the standard quantum limit (SQL) on the measurement precision. When the state is the maximally entangled state then $\chi^2 = 1/N$, which indicates that this can provide the Heisenberg limit (HL).[10,11,37]

2.2. Spin squeezing

Below, we introduce two popular spin squeezing parameters: ξ_{K}^2, as proposed by Kitagawa and Ueda in analogy to photon squeezing,[22] and ξ_{W}^2, as proposed by Wineland in Ramsey experiments.[19] In general, ξ_{K}^2 is not metrologically relevant, while ξ_{W}^2 is. In addition, there are various definitions of spin squeezing that were introduced for certain considerations, and one can refer to Ref. [20] for a detailed discussion.

The two spin squeezing parameters are defined as follows:[19,22]

$$\xi_{\mathrm{K}}^2 = \frac{2\min(\Delta J_{\boldsymbol{n}_\perp}^2)}{N}, \quad \xi_{\mathrm{W}}^2 = \frac{N\min(\Delta J_{\boldsymbol{n}_\perp}^2)}{|\langle J_{\mathrm{n}}\rangle|^2}, \tag{18}$$

where the subscript $\boldsymbol{n}_\perp$ denotes the axis perpendicular to the mean spin, which is given by $\langle \boldsymbol{J}\rangle = \left(\langle J_x\rangle, \langle J_y\rangle, \langle J_z\rangle\right)$. In what follows, we use $V_\pm$ to denote the maximal and minimal variances of $J_{\boldsymbol{n}_\perp}$; namely, $V_+ = \max(J_{\boldsymbol{n}_\perp})$ and $V_- = \min(J_{\boldsymbol{n}_\perp})$. Evidently, these two parameters satisfy the following relations

$$\xi_{\mathrm{W}}^2 = \frac{N^2}{2|\langle J_{\boldsymbol{n}}\rangle|^2}\xi_{\mathrm{K}}^2, \quad \text{and} \quad \xi_{\mathrm{W}}^2 < \xi_{\mathrm{K}}^2. \tag{19}$$

According to the definition of spin squeezing, when a state satisfies the inequality $\xi_i^2 < 1$ $(i = \mathrm{K},\mathrm{W})$, then it is the SSS. This means that, for SSS, its fluctuation of the collective angular momentum is squeezed in one direction and inflated in the another direction, and the fluctuation in the squeezed direction is smaller than the sub-short limit. It has been demonstrated that spin squeezing is aroused from quantum correlation effect among individual particles.[22] One of the main applications of the SSSs is used to reduce quantum noise and increase the signal-to-noise ratio in spectroscopy.[18,19,42,43]

3. The maximal QFI and spin squeezing in the OAT model

In this section, we compare the two quantities: the APEP χ^2 and spin squeezing parameter in the OAT model with an initial CSS $|\theta_0,\phi_0\rangle$ in the absence of noise. Due to the Kitagawa & Ueda spin-squeezing parameter ξ_{K}^2 being not metrologically relevant, we only concentrate on the Wineland spin-squeezing parameter ξ_{W}^2 in what follows. A detailed discussion for the two spin squeezing parameters in the OAT model can be found in Ref. [23]. Below, we first introduce the OAT model, then derive the analytical expression of the maximal QFI in this model, and finally make a comparison between the APEP χ^2 and spin squeezing parameter ξ_{W}^2.

3.1. One-axis twisting model

The Hamiltonian of the OAT model is represented by

$$H = \kappa J_z^2, \tag{20}$$

where κ denotes constant number related to the specific systems.[22] This model has been experimentally realized in both two-mode Bose–Einstein condensates (BECs)[44–46] and light-ensemble interaction in optical cavity.[47] The corresponding time evolution operator to Eq. (20) reads

$$U(t) = \exp(-\mathrm{i}Ht) = \exp\left(-\mathrm{i}\kappa J_z^2 t\right). \tag{21}$$

Generally, the system is initially prepared in a CSS as

$$\begin{aligned}|\theta_0,\phi_0\rangle &\equiv |\theta_0,\phi_0\rangle_k^{\otimes N} \\ &= \left(\cos\frac{\theta_0}{2}|\uparrow\rangle_k + \mathrm{e}^{\mathrm{i}\phi_0}\sin\frac{\theta_0}{2}|\downarrow\rangle_k\right)^{\otimes N},\end{aligned} \tag{22}$$

for $k = 1,2,\ldots,N$, which represents as a product state with a set of N elementary spins all pointing in the same direction (θ_0,ϕ_0). In the above equation, θ_0 and ϕ_0 denote the polar and azimuth angles of the polarization of the spins, respectively. By expanding in the basis of the J_z operator, the CSS of Eq. (22) can be re-expressed as

$$|\theta_0,\phi_0\rangle = \sum_{m=-j}^{j} c_m(0)|j,m\rangle, \tag{23}$$

with the amplitudes

$$\begin{aligned}c_m(0) = &\binom{2j}{j-m}^{1/2}\left(\sin\frac{\theta_0}{2}\right)^{j-m} \\ &\times\left(\cos\frac{\theta_0}{2}\right)^{j+m}\mathrm{e}^{\mathrm{i}(j-m)\phi_0}.\end{aligned} \tag{24}$$

Under the nonlinear evolution of Eq. (21), the state of the system at time t becomes

$$|\psi(t)\rangle = U(t)|\theta_0,\phi_0\rangle = \sum_{m=-j}^{j} c_m(0)\exp\left(-\mathrm{i}\kappa m^2 t\right)|j,m\rangle. \tag{25}$$

Below, we will calculate the maximal QFI $\mathcal{F}_{\varphi,\max}$ for this state.

3.2. The exact solution of the QFI in OAT model

In the Heisenberg picture, with Eq. (21), the time evolution of the ladder operator J_+ could be exactly calculated

$$\tilde{J}_+ = U(t)^\dagger J_+ U(t) = J_+ \exp\left[\mathrm{i}\mu\left(J_z + \frac{1}{2}\right)\right], \tag{26}$$

where the superscript tilde signs that the operator is time-dependent and $\mu = 2\kappa t$. Then we can analytically derive a set of expectations $\langle\tilde{J}_+\rangle, \langle\tilde{J}_+^2\rangle$, and $\langle\tilde{J}_+(\tilde{J}_z + \frac{1}{2})\rangle$ for the OAT-induced state of Eq. (25). The detailed derivation is presented in Appendix A. With Eq. (A1), one can easily obtain the following equations

$$\langle\tilde{J}_x\rangle = \mathrm{Re}\langle\tilde{J}_+\rangle, \text{ and } \langle\tilde{J}_y\rangle = \mathrm{Im}\langle\tilde{J}_+\rangle. \tag{27}$$

Considering the commute relations $[H, J^2] = [H, J_z] = 0$, one readily derives

$$\langle\tilde{J}_z\rangle = \langle J_z\rangle = j\cos\theta_0, \tag{28}$$

$$\langle\tilde{J}_z^2\rangle = \langle J_z^2\rangle = \frac{j}{2} + j\left(j - \frac{1}{2}\right)\cos^2\theta_0, \tag{29}$$

$$\langle\tilde{\boldsymbol{J}}^2\rangle = j(j+1). \tag{30}$$

Now, we choose the new orthogonal vectors as

$$\boldsymbol{n}_1 = (-\sin\phi, \cos\phi, 0), \tag{31}$$

$$\boldsymbol{n}_2 = (-\cos\theta\cos\phi, -\cos\theta\sin\phi, \sin\theta), \tag{32}$$

$$\boldsymbol{n}_3 = (\sin\theta\cos\phi, \sin\theta\sin\phi, \cos\theta), \tag{33}$$

where $\boldsymbol{n}_3$ is the mean spin direction, $\boldsymbol{n}_1$ and $\boldsymbol{n}_2$ are the other two directions perpendicular to $\boldsymbol{n}_3$, and the trigonometric functions are resolved by

$$\cos\theta = \langle\tilde{J}_z\rangle/\mathcal{R}, \ \sin\theta = r/\mathcal{R}, \text{ and } \tan\phi = \langle\tilde{J}_y\rangle/\langle\tilde{J}_x\rangle, \tag{34}$$

with the length of the mean spin

$$\mathcal{R} = |\langle\tilde{\boldsymbol{J}}\rangle| = \sqrt{\langle\tilde{J}_x\rangle^2 + \langle\tilde{J}_y\rangle^2 + \langle\tilde{J}_z\rangle^2}, \tag{35}$$

and

$$r = \mathcal{R}\sin\theta = \sqrt{\langle\tilde{J}_x\rangle^2 + \langle\tilde{J}_y\rangle^2}. \tag{36}$$

It is easy to verify that $\langle J_{\boldsymbol{n}_1}\rangle = \langle J_{\boldsymbol{n}_2}\rangle = 0$ and $\langle J_{\boldsymbol{n}_3}\rangle = |\langle\tilde{\boldsymbol{J}}\rangle|$.

To calculate $\mathcal{F}_{\varphi,\max}$, we first should determine the symmetry covariance matrix $\boldsymbol{C}$ of Eq. (11). In the new orthogonal basis $(\boldsymbol{n}_1, \boldsymbol{n}_2, \boldsymbol{n}_3)$, the matrix $\boldsymbol{C}$ is given by

$$\boldsymbol{C} = \begin{bmatrix} \langle J_{\boldsymbol{n}_1}^2\rangle & \langle[J_{\boldsymbol{n}_1}, J_{\boldsymbol{n}_2}]_+\rangle & \langle[J_{\boldsymbol{n}_1}, J_{\boldsymbol{n}_3}]_+\rangle \\ \langle[J_{\boldsymbol{n}_1}, J_{\boldsymbol{n}_2}]_+\rangle & \langle J_{\boldsymbol{n}_2}^2\rangle & \langle[J_{\boldsymbol{n}_2}, J_{\boldsymbol{n}_3}]_+\rangle \\ \langle[J_{\boldsymbol{n}_1}, J_{\boldsymbol{n}_3}]_+\rangle & \langle[J_{\boldsymbol{n}_2}, J_{\boldsymbol{n}_3}]_+\rangle & \langle J_{\boldsymbol{n}_3}^2\rangle - \langle J_{\boldsymbol{n}_3}\rangle^2 \end{bmatrix}, \tag{37}$$

where the matrix elements of $\boldsymbol{C}$ are fully determined by six terms: $\langle\tilde{\boldsymbol{J}}^2\rangle$, $\langle\tilde{J}_z\rangle$, $\langle\tilde{J}_z^2\rangle$, $\langle\tilde{J}_+\rangle\mathrm{e}^{-\mathrm{i}\phi}$, $\langle\tilde{J}_+^2\rangle\mathrm{e}^{-\mathrm{i}2\phi}$, and $\langle\tilde{J}_+(2\tilde{J}_z + 1)\rangle\mathrm{e}^{-\mathrm{i}\phi}$ (see Table 1). Diagonalize $\boldsymbol{C}$ and find the maximal eigenvalue of $\boldsymbol{C}$ as $\lambda_{\max}$. Then we have

$$\mathcal{F}_{\varphi,\max}(t) = 4\lambda_{\max}. \tag{38}$$

It deserves to noted that all matrix elements of $\boldsymbol{C}$ are independent of ϕ_0. This means that the maximal QFI $\mathcal{F}_{\varphi,\max}(t)$ does not depend on ϕ_0, which is the same as the spin squeezing parameters.[23] This result can be easily understood by considering the commute relation $[H, J_z] = 0$ and the unitary invariance property of the QFI, which states that the value of the QFI remains invariant under the unitary evolution independent of φ.[2,3] Due to the system Hamiltonian commuting with J_z, we have $[R(\phi_0, J_z), U(t)] = 0$, where $R(\phi_0, J_z)$ denotes a rotation around x axis by angle ϕ_0. Then, the OAT-induced state of Eq. (25) satisfies the following chain equalities

$$\begin{aligned} |\psi(t)\rangle &= U(t)|\theta_0, \phi_0\rangle = U(t)R(\phi_0, J_z)|\theta_0, 0\rangle \\ &= R(\phi_0, J_z)U(t)|\theta_0, 0\rangle. \end{aligned} \tag{39}$$

According to the unitary invariance property, the QFI of the state $U(t)|\theta_0, \phi_0\rangle$ equals that of the state $U(t)|\theta_0, 0\rangle$, which is ϕ_0-independent. Thus, this means that the QFI is ϕ_0-independent. In what follows, we set $\phi_0 = 0$ as the initial CSS.

Table 1. The matrix elements of the symmetry covariance matrix $\boldsymbol{C}$ of Eq. (37) are fully represented by six terms: $\langle\tilde{\boldsymbol{J}}^2\rangle$, $\langle\tilde{J}_z\rangle$, $\langle\tilde{J}_z^2\rangle$, $\langle\tilde{J}_+\rangle\mathrm{e}^{-\mathrm{i}\phi}$, $\langle\tilde{J}_+^2\rangle\mathrm{e}^{-\mathrm{i}2\phi}$, and $\langle\tilde{J}_+(2\tilde{J}_z+1)\rangle\mathrm{e}^{-\mathrm{i}\phi}$.

$\langle J_{\boldsymbol{n}_3}\rangle$	$\sin\theta\,\mathrm{Re}[\langle\tilde{J}_+\rangle\mathrm{e}^{-\mathrm{i}\phi}] + \cos\theta\,\langle\tilde{J}_z\rangle$
$\langle J_{\boldsymbol{n}_1}^2\rangle$	$\frac{1}{2}[\langle\tilde{\boldsymbol{J}}^2\rangle - \langle\tilde{J}_z^2\rangle] - \frac{1}{2}\mathrm{Re}[\langle\tilde{J}_+^2\rangle\mathrm{e}^{-\mathrm{i}2\phi}]$
$\langle J_{\boldsymbol{n}_2}^2\rangle$	$\frac{1}{2}\cos^2\theta[\langle\tilde{\boldsymbol{J}}^2\rangle - \langle\tilde{J}_z^2\rangle] + \sin^2\theta\langle\tilde{J}_z^2\rangle + \frac{1}{2}\cos^2\theta\,\mathrm{Re}[\langle\tilde{J}_+^2\rangle\mathrm{e}^{-\mathrm{i}2\phi}] - \frac{1}{2}\sin 2\theta\,\mathrm{Re}[\langle\tilde{J}_+(2\tilde{J}_z+1)\rangle\mathrm{e}^{-\mathrm{i}\phi}]$
$\langle J_{\boldsymbol{n}_3}^2\rangle$	$\frac{1}{2}\sin^2\theta[\langle\tilde{\boldsymbol{J}}^2\rangle - \langle\tilde{J}_z^2\rangle] + \cos^2\theta\langle\tilde{J}_z^2\rangle + \frac{1}{2}\sin^2\theta\,\mathrm{Re}[\langle\tilde{J}_+^2\rangle\mathrm{e}^{-\mathrm{i}2\phi}] + \frac{1}{2}\sin 2\theta\,\mathrm{Re}[\langle\tilde{J}_+(2\tilde{J}_z+1)\rangle\mathrm{e}^{-\mathrm{i}\phi}]$
$\langle[J_{\boldsymbol{n}_1}, J_{\boldsymbol{n}_2}]_+\rangle$	$-\cos\theta\,\mathrm{Im}[\langle\tilde{J}_+^2\rangle\mathrm{e}^{-\mathrm{i}2\phi}] + \sin\theta\,\mathrm{Im}[\langle\tilde{J}_+(2\tilde{J}_z+1)\rangle\mathrm{e}^{-\mathrm{i}\phi}]$
$\langle[J_{\boldsymbol{n}_1}, J_{\boldsymbol{n}_3}]_+\rangle$	$\sin\theta\,\mathrm{Im}[\langle\tilde{J}_+^2\rangle\mathrm{e}^{-\mathrm{i}2\phi}] + \sin\theta\,\mathrm{Im}[\langle\tilde{J}_+(2\tilde{J}_z+1)\rangle\mathrm{e}^{-\mathrm{i}\phi}]$
$\langle[J_{\boldsymbol{n}_2}, J_{\boldsymbol{n}_3}]_+\rangle$	$-\frac{1}{2}\sin 2\theta[\langle\tilde{\boldsymbol{J}}^2\rangle - 3\langle\tilde{J}_z^2\rangle + \langle\tilde{J}_+^2\rangle\mathrm{e}^{-\mathrm{i}2\phi}] - \cos 2\theta\,\mathrm{Re}[\langle\tilde{J}_+(2\tilde{J}_z+1)\rangle\mathrm{e}^{-\mathrm{i}\phi}]$

The above derivation of the maximal QFI involves the diagonalization of the matrix $\boldsymbol{C}$. This indicates that $\mathcal{F}_{\varphi,\max}$ corresponds to the maximal variance of the angular momentum operator in the coordinate sphere. Now, we only focus on the maximal and minimal variances in the plane perpendicular to the mean spin direction. We introduce a component of the collective angular momentum normal to the mean spin direction as

$$J_{\boldsymbol{n}_\perp} = \mathrm{e}^{-\mathrm{i}\vartheta J_{\boldsymbol{n}_3}} J_{\boldsymbol{n}_1} \mathrm{e}^{\mathrm{i}\vartheta J_{\boldsymbol{n}_3}} = J_{\boldsymbol{n}_1}\cos\vartheta + J_{\boldsymbol{n}_2}\sin\vartheta. \quad (40)$$

Due to $\langle J_{\boldsymbol{n}_1}\rangle = \langle J_{\boldsymbol{n}_2}\rangle = 0$, we have $\langle J_{\boldsymbol{n}_\perp}\rangle = 0$. Then, the variance of $J_{\boldsymbol{n}_\perp}$ is[22]

$$\langle \Delta J^2_{\boldsymbol{n}_\perp}\rangle = \langle J^2_{\boldsymbol{n}_\perp}\rangle = \frac{1}{2}[\mathcal{C} + \sqrt{\mathcal{A}^2+\mathcal{B}^2}\cos(2\vartheta - 2\delta)], \quad (41)$$

with $\tan 2\delta = \mathcal{B}/\mathcal{A}$, where the coefficients

$$\mathcal{A} = \langle J^2_{\boldsymbol{n}_1} - J^2_{\boldsymbol{n}_2}\rangle, \mathcal{B} = \langle [J_{\boldsymbol{n}_1}, J_{\boldsymbol{n}_2}]_+\rangle$$

and

$$\mathcal{C} = \langle J^2_{\boldsymbol{n}_1} + J^2_{\boldsymbol{n}_2}\rangle = j(j+1) - \langle J^2_{\boldsymbol{n}_3}\rangle,$$

(see Table 1). The maximal and minimal fluctuations are expressed as

$$V_\pm = (\mathcal{C} \pm \sqrt{\mathcal{A}^2+\mathcal{B}^2})/2, \quad (42)$$

where V_+ occurs along the optimal anti-squeezed angle as $\vartheta_{\mathrm{op}} = \left[\tan^{-1}(\mathcal{B}/\mathcal{A})\right]/2$ and V_- along the optimal squeezed angle as $\vartheta_{\mathrm{op}} = \left[\tan^{-1}(\mathcal{B}/\mathcal{A}) + \pi\right]/2$. It has been numerically found that the maximal QFI for OAT-induced state is[25]

$$\mathcal{F}_{\varphi,\max}(t) = 4\max\{V_+, \Delta J^2_{\boldsymbol{n}_3}\}. \quad (43)$$

For odd values of N, $\mathcal{F}_{\varphi,\max}$ always occurs in the $\boldsymbol{n}_1\boldsymbol{n}_2$-plane; that is, $\mathcal{F}_{\varphi,\max}(t) = 4V_+$. For even N when $\Delta J^2_{\boldsymbol{n}_3} = V_+$, $\mathcal{F}_{\varphi,\max}$ occurs in the $\boldsymbol{n}_3$ direction.[25]

3.3. A comparison of the parameters between χ^2 and ξ^2_{W}

Figure 1(a) displays the dynamics of χ^2 and ξ^2_{W} versus time for the OAT-induced state of Eq. (25) in terms of two different initial CSSs $|\theta_0 = \pi/2, \phi_0 = 0\rangle$ and $|\pi/3, 0\rangle$. This shows that ξ^2_{W} obviously changes when θ_0 varies from $\pi/2$ to $\pi/3$. Meanwhile, we see that both the time intervals during which squeezing occurs and the degree of squeezing are shrunken. In contrast from the behavior of ξ^2_{W}, χ^2 is rather stable, only having a small amount of reduction when θ_0 changes from $\pi/2$ to $\pi/3$. As shown in Figs. 1(a) and 2(b) for a total time period, χ^2 decreases quickly from the initial value of 1 at beginning, then reaches a plateau ($\chi^2 \propto 2/N$) in the time interval of $3/\sqrt{N} \le \kappa t \le \pi/2 - 3/\sqrt{N}$, and arrives its minimal value at time point of $\kappa t = \pi/2$.[10] For the case of $\theta_0 = \pi/2$, the minimal value of χ^2 at $\kappa t = \pi/2$ corresponds to the HL $1/N$. More importantly, when $\xi^2_{\mathrm{W}} \ge 1$, which indicates that the state is no-squeezed, we still have $\chi^2 < 1$, which means this state is entangled and helpful for improvement of APEP.[10] Since χ^2 stays on the plateau for quite a long time, this means that one can acquire a near-Heisenberg limit $\propto 2/N$ with the OAT-induced state only at the expense of a bit precision.

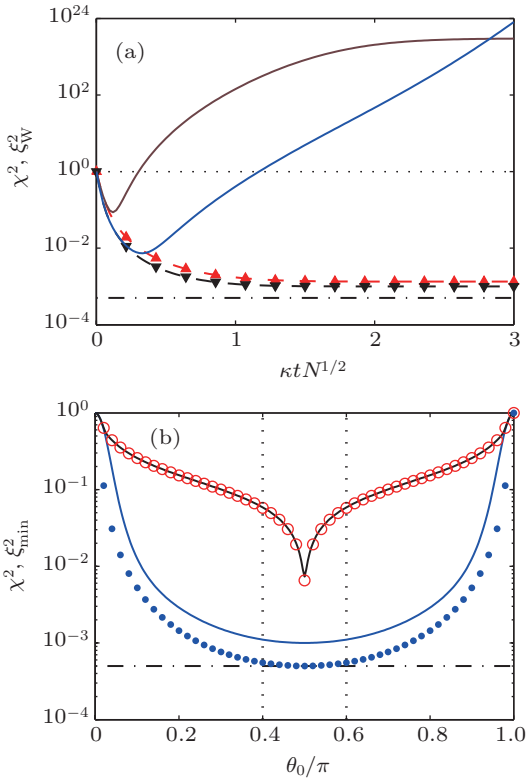


Fig. 1. (color online) (a) Plots of ξ^2_{W} (solid lines) and χ^2 (dashed lines) in terms of the re-scaled time $\kappa t\sqrt{N}$ with $N = 2\times 10^3$ for two different initial CSSs: $|\pi/2, 0\rangle$ (black and blue) and $|\pi/3, 0\rangle$ (red and brown). Upward triangle and downward triangle are plotted by $\chi^2 = N/4V_+$ from Eq. (43). (b) Plots of the minimum value of parameters: $\xi^2_{\mathrm{K,min}}$ (red circles)[23] and χ^2_{min} (blue dots) in terms of θ_0 for $N = 2\times 10^3$. Black soiled curve denotes $\xi^2_{\mathrm{W,min}}$.[23] Solid blue curve denotes the value of χ^2 at $\kappa t = 3/\sqrt{N}$ (being on the plateau in Fig. 1(a)). In both panels (a) and (b), dot–dashed black lines represent the fundamental HL $1/N$.

In Fig. 1(b), we plot χ^2_{min} and ξ^2_{min} as the function of θ_0. We also plot χ^2 (solid blue curve) at $\kappa t = 3/\sqrt{N}$ (being on the plateau in Fig. 1(b)) versus θ_0. This clearly shows that both the strongest squeezing and the best APEP occur for $\theta_0 = \pi/2$. However, when θ_0 slightly deviates from the optimal value of $\pi/2$, the degree of squeezing is decreased. In contrast from the behavior of ξ^2_{min}, χ^2 is fairly robust against θ_0 in the vicinity of $\theta_0 = \pi/2$. We see that χ^2 is stable in the regime of $|\theta_0 - \pi/2| < 2\pi/5$, as marked by vertical dotted lines.

The fact is that the ideal optimal CSS $|\pi/2, 0\rangle$ is hard to generate in experiment. It is experimentally shown that 98% of the atoms can be prepared in the ideal state through optical pumping at present.[31] According to χ^2, we find that the accuracy of estimation given by the state nonlinearly evolved

from an unideal initial CSS $\theta_0 \sim \pi/2$ is almost the same as the sensitivity given by the OAT-induced state from the optimal CSS.

4. The maximal QFI and spin squeezing under collective dephasing

Up to now, we have not considered the influences of decoherence on the dynamics of χ^2 and ξ_W^2 in the OAT model. In the real experiment, the collective dephasing process always exists due to the interaction between the atoms and thermal reservoir in a two component atomic BEC system. Then, the time evolution of the system is governed by the following master equation[6,33–35]

$$\dot{\rho}(t) = \mathrm{i}[\rho, \kappa J_z^2] + \mathcal{L}\rho, \tag{44}$$

with

$$\mathcal{L}\rho \equiv \Gamma(2J_z\rho(t)J_z - \rho(t)J_z^2 - J_z^2\rho(t)), \tag{45}$$

where $\mathcal{L}$ denotes the Lindblad superoperator, Γ denotes the dephasing rate, and ρ denotes the reduced density operator of the system in the interaction picture. Here, as is shown in Eq. (44), we have assumed that the processes is Markovian. From Eq. (44), the time evolutions of the density matrix elements are given as follows:

$$\begin{aligned}\rho_{m,n}(t) &\equiv \langle j,m|\rho(t)|j,n\rangle \\ &= \rho_{m,n}(0)\exp[\mathrm{i}(n^2-m^2)\tau - (m-n)^2\gamma\tau],\end{aligned} \tag{46}$$

where we set $\tau = \kappa t$ and $\gamma = \Gamma/\kappa$. Equation (46) shows that collective dephasing makes the diagonal elements of the density matrix unchanged and energy-conserved. Here, we assume that the dephasing is introduced on the state preparation and the eventual interferometer that comes after the state preparation is noiseless.

In this case, ξ_W^2 can be exactly solved. Here, the state of system is denoted by the density matrix of Eq. (46). Then we find that $\langle \tilde{J}_+ \rangle$, $\langle \tilde{J}_+(\tilde{J}_z + \frac{1}{2})\rangle$, and $\langle \tilde{J}_+^2 \rangle$ equal Eqs. (A1), (A5), and (A6) by multiplying the factors of $\mathrm{e}^{-\gamma\tau}$, $\mathrm{e}^{-4\gamma\tau}$, and $\mathrm{e}^{-\gamma\tau}$, respectively. Due to $[J^2, \mathcal{L}] = [J_z, \mathcal{L}] = 0$, the expressions of $\langle \tilde{J}^2 \rangle$, $\langle \tilde{J}_z \rangle$, and $\langle \tilde{J}_z^2 \rangle$ remain unchanged, as given by Eqs. (30), (28), and (29). By submitting those solutions into Eq. (42), one can exactly obtain V_- and ξ_W^2 with Eq. (18). The APEP χ^2 for the state of Eq. (46) can be numerically calculated based on Eqs. (8) and (9). Here, we note that both the spin squeezing parameter ξ_W^2 and the QFI are independent of the initial azimuth angle ϕ_0.

In Figs. 2(a) and 2(b), we plot the time evolutions of ξ_W^2 and χ^2 in terms of different decay rates $\gamma = 0$, 0.01, and 0.1 for the ideal initial CSS $\theta_0 = \pi/2$. As shown in Fig. 2(a), the degree of squeezing is weakened as γ increases, while the time interval of squeezing remains unchanged for different values of γ. Fig. 2(b) shows that the symmetry of χ^2 is broken in the presence of collective dephasing. With the strength of the decay rate increasing, the Heisenberg-scaling-limit precision cannot be obtained. However, the plateau always exists, even for the strong decay rate $\gamma = 0.1$, only with the time at which χ^2 arrives the plateau delayed. This means that one can still acquire the near-Heisenberg limit by extending the evolution time. A related work in Ref. [36] investigated the effect of phase noise on quantum correlations in two-mode Bose–Josephson junctions and analyzed its effect on squeezed states generated from the ideal initial CSS $\theta_0 = \pi/2$. Here, our results are consistent with that given in Ref. [36].

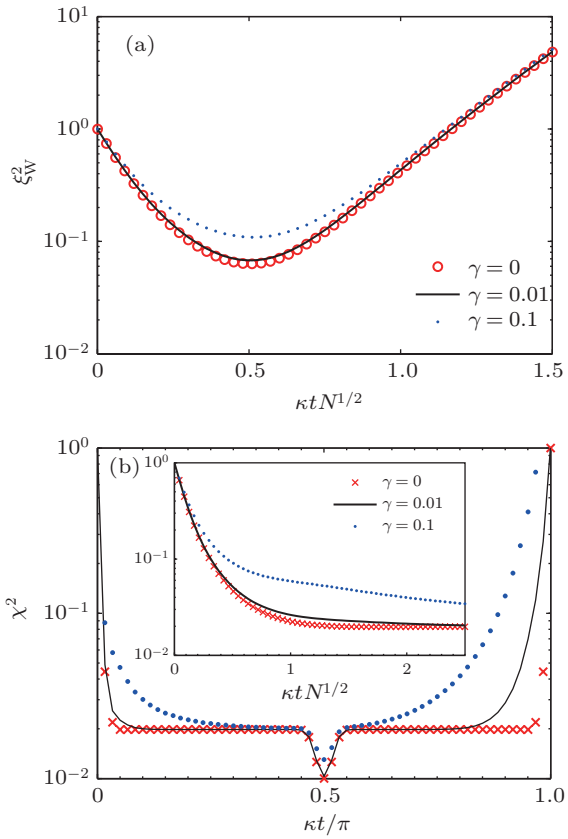


Fig. 2. (color online) Plots of the time evolution of ξ_W^2 (a) and χ^2 (b) with $N = 100$ for $\theta_0 = \pi/2$ in terms of three cases: $\gamma = 0$, 0.01, and 0.1. (b) Plots of χ^2 for a period of time $\kappa T = \pi$ and inset is plotted for a short time range.

5. Conclusion

We have studied the dependence of the APEP χ^2[10] on the polar angle of the initial CSS $|\theta_0, \phi_0\rangle$ in the OAT model. In Ref. [23], it has been found that spin squeezing depends sensitively on the polar angle θ_0 of the initial CSS and the degree of spin squeezing degrades significantly when θ_0 slightly deviates from the optimal angle $\pi/2$. We show that χ^2 is insensitive to the angle θ_0 in the vicinity of $\pi/2$. Meanwhile, we find that χ^2 is quite stable during the time evolution. In the time scales of $1/\sqrt{N} \leq \kappa t < \pi/2 - 1/\sqrt{N}$ with $N = 2 \times 10^3$,

χ^2 always stays on the plateau level of 10^{-3} dB. Our results indicate that the OAT-induced states from non-ideal initial CSSs $\theta_0 \sim \pi/2$ can still acquire a near-Heisenberg-scaling precision $\propto 2/N$ for quantum single-parameter estimation. The common feature of ξ_W^2 and χ^2 is that they are independent of the azimuth angle ϕ_0 of the initial CSS.

Additionally, we considered the effects of the collective dephasing on the dynamics of ξ_W^2 and χ^2. The analytical expression of ξ_W^2 was obtained and χ^2 was numerically calculated. As the strength of the decay rate γ increases, the degree of the maximal spin squeezing decreases obviously; however, the time interval of squeezing remains unchanged. More importantly, our results show that by extending the evolution time χ^2 can still reach the near-Heisenberg limit, even in the presence of collective dephasing. Our work can have a practical impact on precision estimation in quantum metrology with the OAT-induced state and can be implemented with BECs within current technology.

Appendix A: Calculation of expectations of the spin components

In this appendix, we derive some formulas for calculating the expectations of the angular momentum. A coherent spin state $|\theta_0, \phi_0\rangle$ can be expressed in the form of Eq. (23). The expectations of the spin components in Table 1 are calculated from

$$\langle \tilde{J}_+ \rangle = j \sin\theta_0 \, \mathrm{e}^{\mathrm{i}\phi_0} \left(\cos\frac{\mu}{2} + \mathrm{i}\cos\theta_0 \sin\frac{\mu}{2} \right)^{2j-1}, \tag{A1}$$

which can readily be rewritten as

$$\langle \tilde{J}_+ \rangle = r \exp(\mathrm{i}\phi), \tag{A2}$$

with the corresponding modulus and argument being

$$r = j \sin\theta_0 \left(1 - \sin^2\theta_0 \sin^2\frac{\mu}{2} \right)^{j-1/2}, \tag{A3}$$

$$\phi = \phi_0 + (2j-1) \arctan\left(\cos\theta_0 \tan\frac{\mu}{2} \right). \tag{A4}$$

Furthermore, we obtain

$$\langle \tilde{J}_+^2 \rangle = j\left(j - \frac{1}{2} \right) \mathrm{e}^{2\mathrm{i}\phi_0} \sin^2\theta_0 \left(\cos\mu + \mathrm{i}\cos\theta_0 \sin\mu \right)^{2j-2}. \tag{A5}$$

Differentiating Eq. (A1) with respect to μ yields

$$\begin{aligned} \langle \tilde{J}_+ (\tilde{J}_z + \frac{1}{2}) \rangle = {} & j\left(j - \frac{1}{2} \right) \sin\theta_0 \, \mathrm{e}^{\mathrm{i}\phi_0} \\ & \times \left(\cos\frac{\mu}{2} + \mathrm{i}\cos\theta_0 \sin\frac{\mu}{2} \right)^{2j-2} \\ & \times \left(\mathrm{i}\sin\frac{\mu}{2} + \cos\theta_0 \cos\frac{\mu}{2} \right). \end{aligned} \tag{A6}$$

References

[1] Fisher R A 1925 *Proc. Cambridge Philos. Soc.* **22** 700
[2] Helstrom C W 1976 *Quantum Detection and Estimation Theory* (New York: Academic Press) p. 268
[3] Holevo A S 1982 *Probabilistic and Statistical Aspects of Quantum Theory* (Amsterdam: North-Holland) p. 276
[4] Braunstein S L and Caves C M 1994 *Phys. Rev. Lett.* **72** 3439
[5] Braunstein S L, Caves C M and Milburn G J 1996 *Ann. Phys.* **247** 135
[6] Zhong W, Sun Z, Ma J, Wang X G and Nori F 2013 *Phys. Rev. A* **87** 022337
[7] Zhang Y Y, Chen Q H and Wang K L 2010 *Phys. Rev. B* **81** 121105
[8] Rivas Á and Luis A 2010 *Phys. Rev. Lett.* **105** 010403
[9] Girolami D, Tufarelli T and Adesso G 2013 *Phys. Rev. Lett.* **110** 240402
[10] Pezze L and Smerzi A 2009 *Phys. Rev. Lett.* **102** 100401
[11] Laskowski P W, Krischek R, Schwemmer C, Wieczorek W, Weinfurter H, Pezze L and Smerzi A 2012 *Phys. Rev. A* **85** 022321
[12] Lu X M, Wang X G and Sun C P 2010 *Phys. Rev. A* **82** 042103
[13] Berrada K 2013 *Phys. Rev. A* **88** 035806
[14] Yan D, Liu Y and Song L J 2011 *Acta Phys. Sin.* **60** 120302 (in Chinese)
[15] Wang X Q, Ma J, Zhang X H and Wang X G 2011 *Chin. Phys. B* **20** 050510
[16] Sun Z, Lu X M and Wang X G 2010 *Phys. Rev. A* **82** 022306
[17] Huang Y X, Zhong W, Sun Z and Wang X G 2012 *Phys. Rev. A* **86** 012320
[18] Wineland D J, Bollinger J J, Itano W M, Moore F L and Heinzen D J 1992 *Phys. Rev. A* **46** R6797
[19] Wineland D J, Bollinger J J, Itano W M and Heinzen D J 1994 *Phys. Rev. A* **50** 67
[20] Ma J, Wang X G, Sun C P and Nori F 2011 *Phys. Rep.* **509** 89
[21] Xue P 2012 *Chin. Phys. B* **21** 100306
[22] Kitagawa M and Ueda M 1993 *Phys. Rev. A* **47** 5138
[23] Jin G R, Liu Y C and Liu W M 2009 *New J. Phys.* **11** 073049
[24] Chen D W, Yan D and Song L J 2009 *Acta Phys. Sin.* **58** 3679 (in Chinese)
[25] Liu W F, Xiong H N, Ma J and Wang X G 2010 *Int. J. Theor. Phys.* **49** 1073
[26] Sun H G, Liu W F and Li C J 2011 *Chin. Phys. B* **20** 090301
[27] Hald J, Sorensen J L, Schori C and Polzik E S 1999 *Phys. Rev. Lett.* **83** 1319
[28] Takeuchi M, Ichihara S, Takano T, Kumakura M, Yabuzaki T and Takahashi Y 2005 *Phys. Rev. Lett.* **94** 023003
[29] Kuzmich A, Mandel L and Bigelow N P 2000 *Phys. Rev. Lett.* **85** 1594
[30] Chaudhury S, Merkel S, Herr T, Silberfarb A, Deutsch I H and Jessen P S 2007 *Phys. Rev. Lett.* **99** 163002
[31] Fernholz T, Krauter H, Jensen K, Sherson J F, Sorensen A S and Polzik E S 2008 *Phys. Rev. Lett.* **101** 073601
[32] Takano T, Fuyama M, Namiki R and Takahashi Y 2009 *Phys. Rev. Lett.* **102** 033601
[33] Khodorkovsky Y, Kurizki G and Vardi A 2009 *Phys. Rev. A* **80** 023609
[34] Liu Y C, Jin G R and You L 2010 *Phys. Rev. A* **82** 045601
[35] Dorner U 2012 *New J. Phys.* **14** 043011
[36] Ferrini G, Spehner D, Minguzzi A and Hekking F W J 2011 *Phys. Rev. A* **84** 043628
[37] Giovannetti V, Lloyd S and Maccone L 2006 *Phys. Rev. Lett.* **96** 010401
[38] Escher B M, de Matos Fillo R L and Davidovich L 2011 *Nat. Phys.* **7** 406
[39] Demkowicz-Dobrzański R, Kołodyński J and Gută M 2012 *Nat. Commun.* **3** 1063
[40] Yurke B, McCall S L and Klauder J R 1986 *Phys. Rev. A* **33** 4033
[41] Hyllus P, Gühne O and Smerzi A 2010 *Phys. Rev. A* **82** 012337
[42] Petrov P G, Oblak D, Alzar C L G, Kjægaard N and Polzik E S 2007 *Phys. Rev. A* **75** 033803
[43] Chaudhury S, Smith G A, Schulz K and Jessen P S 2006 *Phys. Rev. Lett.* **96** 043001
[44] Gross C, Zibold T, Nicklas E, Estève J and Oberthaler M K 2010 *Nature* **464** 1165
[45] Riedel M F, Böhi P, Li Y, Hänsch T W, Sinatra A and Treutlein P 2010 *Nature* **464** 1170
[46] Sϕnsen A, Duan L M, Cirac J I and Zoller P 2001 *Nature* **409** 63
[47] Schleier-Smith M H, Leroux I D and Vuletic V 2010 *Phys. Rev. A* **81** 021804